ELSEVIER

NeuroToxicology 22 (2001) 387–392

NeuroToxicology

Non Invasive Quantification of Manganese Deposits in the Rat Brain by Local Measurement of NMR Proton T_1 Relaxation Times

Bernard Gallez[1,2,*], Roger Demeure[2], Christine Baudelet[1,2], Nadia Abdelouahab[3], Nelson Beghein[2], Bénédicte Jordan[1,2], Muriel Geurts[4], Harry A. Roels[3]

[1]*Laboratory of Medicinal Chemistry and Radiopharmacy, Université catholique de Louvain, B-1200 Brussels, Belgium*
[2]*Laboratory of Biomedical Magnetic Resonance, Université catholique de Louvain, B-1200 Brussels, Belgium*
[3]*Industrial Toxicology and Occupational Medicine Unit, Université catholique de Louvain, B-1200 Brussels, Belgium*
[4]*Laboratory of Pharmacology, Université catholique de Louvain, B-1200 Brussels, Belgium*

Received 21 September 2000; accepted 7 March 2001

Abstract

Up to now, there is no reliable non invasive biomarker for the concentration of manganese (Mn) in the brain after intoxication to this metal. The aim of the present experimental study was to determine the predictive value of the localized measurement of the proton NMR relaxation time T_1 as a quantitative estimation of the concentration of Mn in brain. The relationship of the proton relaxation rates ($1/T_1$) was established in rat brain homogenates as a function of the Mn, iron, and copper concentration. Subsequently, an experimental model of Mn neurotoxicity was used: rats were stereotactically injected with increasing amounts of Mn^{2+} (as $MnCl_2$) in the ventricles. After 3 weeks, local measurements of T_1 were carried out in live rats. They were then sacrificed in order to sample the striatum, the cortex, and the cerebellum from the brain and to perform a quantitative determination of the concentration of Mn in these tissues by atomic absorption spectrometry (AAS). The results indicate excellent correlation coefficients between relaxation rates and tissue Mn concentrations ($r = 0.84$, 0.77 and 0.92 for the striatum, the cortex and the cerebellum, respectively). This methodology offers a unique tool for monitoring the degree of Mn concentration in different areas of the brain in animal models of Mn intoxication. It will be useful for evaluating the efficacy of treatments aimed at decreasing the metal in the brain. The method could be potentially useful for being transposed in the clinical situation for monitoring Mn-exposed workers.

Keywords: Manganese; Neurotoxicity; Brain; T_1; MRI; Rat

INTRODUCTION

Manganese (Mn) is an essential metal of toxicological concern mainly because overexposure may lead to toxic effects in the central nervous system. Manganism consists of behavioral and neurological signs resembling Parkinson's disease. This extrapyramidal toxicity in humans is thought to arise from a disruption of the dopaminergic system mediated by the selective accumulation of Mn in the basal ganglia, especially the corpus striatum (Barbeau, 1984). Mn-linked neuropathology has been diagnosed in subjects chronically exposed to high levels of airborne Mn at the workplace (Huang et al., 1989) and in patients with cirrhosis and/or impaired biliary elimination (Malecki et al., 1999). The early neurobehavioral changes frequently found in Mn workers are currently a matter of concern as to whether they are predictive of irreversible damage (Mergler, 1996; Roels et al., 1992, 1999) and the

* Corresponding author. Tel.: +32-2-7647348; fax: +32-2-7647363.
E-mail address: gallez@cmfa.ucl.ac.be (B. Gallez).

0161-813X/01/$ – see front matter
PII: S0161-813X(01)00020-1

toxicological significance of the injection of Mn-based contrast agents in patients is still debatable (Gallez et al., 1997, 1998).

Up to now, there is no reliable biomarker reflecting the concentration of Mn at critical brain site(s) after intoxication, and the clinical evaluation is based on only signs and symptoms. Previous magnetic resonance (MR) studies described the effect of Mn presence on signal in T_1-weighted images of the brain of primates used for experimental Mn neurotoxicity (Newland and Weiss, 1992; Newland et al., 1989) and in patients, viz. cirrhotic patients (Malecki et al., 1999; Spahr et al., 1996), patients receiving total parenteral nutrition (Mirowitz and Westrich, 1992), and Mn-exposed workers presenting with manganism (Nelson et al., 1993). It was previously shown in animals (Shinotoh et al., 1995; Pautler et al., 1998) and in humans (Hauser et al., 1994; Krieger et al., 1995; Spahr et al., 1996) that the hyperintensities in MR T_1-weighted images of the basal ganglia correlate with the exposure to Mn and the concentration of Mn found in the blood. To describe the extent of intoxication using T_1-weighted images, several authors used the 'pallidal index' (PI: ratio of the globus pallidus signal intensity to the subcortical frontal white matter signal intensity) (Krieger et al., 1995; Spahr et al., 1996). However, the value of the PI cannot be directly related to a local concentration of Mn. Therefore, T_1-weighted imaging should be considered as a qualitative marker and not as a quantitative marker of Mn intoxication. Recently, in a limited number of samples (four rabbits), Kim et al. (1999) suggested that the use of T_1 could be a more reliable measurement of the local Mn concentration in the brain, instead of using other derived expressions. The aim of the present study was to evaluate in large number of intoxicated animals (29 rats) the value of localized measurements of the proton spin-lattice relaxation times (T_1) in different parts of the brain as a quantitative biomarker of Mn deposited in these tissues. We first evaluated the effect of the concentration of Mn, iron, and copper on the proton T_1 measured in rat brain homogenates. In order to demonstrate the usefulness of the measurement of T_1 as a quantitative biomarker of Mn deposits, we carried out a study using an experimental rat model of Mn neurotoxicity. Rats were stereotactically injected with increasing amounts of Mn^{2+} in the brain ventricles. After 3 weeks, the time necessary to get uniform distribution of Mn in the different regions of the brain, local measurements of T_1 were carried out in live rats. They were then sacrificed in order to sample different brain regions of interest (ROI) and to perform a quantitative determination of the concentration of Mn by atomic absorption spectrometry (AAS).

MATERIAL AND METHODS

Metal-Doped Rat Brain Homogenates

The influence of Mn^{2+}, Fe^{3+}, and Cu^{2+} ions on relaxation time T_1 was studied in brain homogenates. Rats were sacrificed by decapitation and the brain was removed from the skull. The brain homogenates were obtained by adding an equivalent amount (w/w) of PBS buffer (pH = 7.4) and using a Potter–Elvehjem homogenizer. Increasing amounts of Mn^{2+}, Fe^{3+}, Cu^{2+} were added to the homogenates to get variable concentrations of metal ions up to 0.4 mmol/l.

Rat Model for Mn Neurotoxicity

The 29 male Wistar rats (250–300 g, Animalerie Facultaire UCL, Brussels) used in this study were anesthetized by i.p. injection of chloral hydrate (6 g/100 ml, 6 ml/kg) and stereotactically injected with saline (nine rats) or increasing amounts of Mn into the ventricles at stereotactic coordinates measured from Bregma: lat. = +1.3 mm, ant. = −0.8 mm, depth = 3.5 mm. A volume of 10 μl of saline (0.9%, w/v) or Mn^{2+} solution with variable concentrations of $MnCl_2$ (ranging from 10 to 100 mmol Mn/l), were injected using a Harvard Pump (rate of injection: 1 μl/min; 5 min rest before removing the needle). Three weeks after the injection (time necessary to allow diffusion of Mn into the different parts of the brain and to get uniform signal intensity in MR images of these regions), NMR studies were carried out on the rats anesthetized by i.p. injection of chloral hydrate.

NMR Measurements

Scans were performed with a 4.7 T Bruker Biospec (Bruker, Ettlingen, Germany) imager equipped with a 40 cm inner diameter (i.d.) bore and a 12 cm shielded gradient hardware (rise time 80 μs; maximum gradient strength = 200 mT/m). Images were obtained in a linearly polarized 'bird cage' transmitter–receiver coil, 70 mm i.d. Gaussian-shaped resonance frequency (RF) pulses (width = 2 ms) were applied for both magnetization–excitation and inversion. The spectral width (SW) was set to 71 kHz. In order to maintain the brain homogenates and rats at a constant temperature of

$37 \pm 2^{\circ}C$, a microprocessor-controlled air warming system was used to blow a warm air flow inside the magnet tunnel. For both in vitro and in vivo experiments, T_1 relaxation time measurements were performed using image series that we named "T_1 calculated images". They were acquired with a modification of a regular multi-slice multi-echo (MSME) pulse sequence to allow data acquisitions with variable repetition time (TR) for which imaging preparation parameters (shimming, receiver gain, RF gains and RF) were kept unchanged. Eight different TRs ranging from 100 ms to 7 s were used to cover the full T_1 recovery range of brain tissues. Images were processed using an in-house program based on the interactive display language (IDL, Boulder Co.) development software running on a PC-Pentium computer. ROI were manually selected and the average pixel intensity was calculated for each TR value. To calculate the T_1 relaxation time, these data were fitted with a standard two-parameter single exponential decay function of the form: $I = I_0 \times [1 - \exp(-\mathrm{TR}/T_1)]$, where I_0 is the initial signal intensity which depends on the proton density and the machine settings, TR the repetition time, and T_1 the relaxation time under investigation. The non-linear fitting of the experimental data to this equation was realized using a general non-linear Levenberg–Marquardt algorithm which is included in the IDL library. The acquisition parameters of the "T_1 calculated images" were echo time (TE) = 10 ms, slice thickness (ST) = 2 mm, number of averages (NA) = 2, field of view (FOV) = 45 mm, and matrix size = 64^2, leading to an approximated total acquisition time of 40 min. For in vivo studies, a fast spin echo (RARE) pulse sequence was used both for localization and high resolution of anatomical images. From a set of four contiguous T_2-weighted sagittal slices of 2 mm thickness, two T_2-weighted transverse slices were selected at the level of the brain regions to be examined. TR, echo train length (ETL), ST, NA, FOV, matrix size, and TE of the anatomical images were 3000 ms; 8, 2 mm; 8, 45 mm; 128^2 and 13 ms, respectively, giving an effective echo time (TE_{eff}) of 52 ms. To maintain the same image matrix size (128^2) and consequently the same in-plane spatial resolution (350 mm/pixel) between the T_2-weighted anatomical images and the "T_1 calculated images", the raw data of the "T_1 calculated images" were zero-filled in the k-space along both frequency and phase encoding directions before the application of the 2D-FFT operator. To evaluate the signal intensities of the tissue of interest against TR, polygonal ROIs in the striatum, cortex, and cerebellum were drawn by hand in the anatomical slices and next copied in the "T_1 calculated images" (Fig. 1). The T_1 relaxation times were determined in the striatum, the frontal and parietal cortex, and the cerebellum. After the NMR study, the animals were sacrificed, the brain removed from the skull, and the striatum, cortex, and cerebellum dissected from the brain with stainless steel surgical instruments for subsequent Mn analysis using AAS.

Atomic Absorption Spectrometric Measurements

The freshly dissected cerebellum and cortex tissues were first cut in small pieces with stainless steel

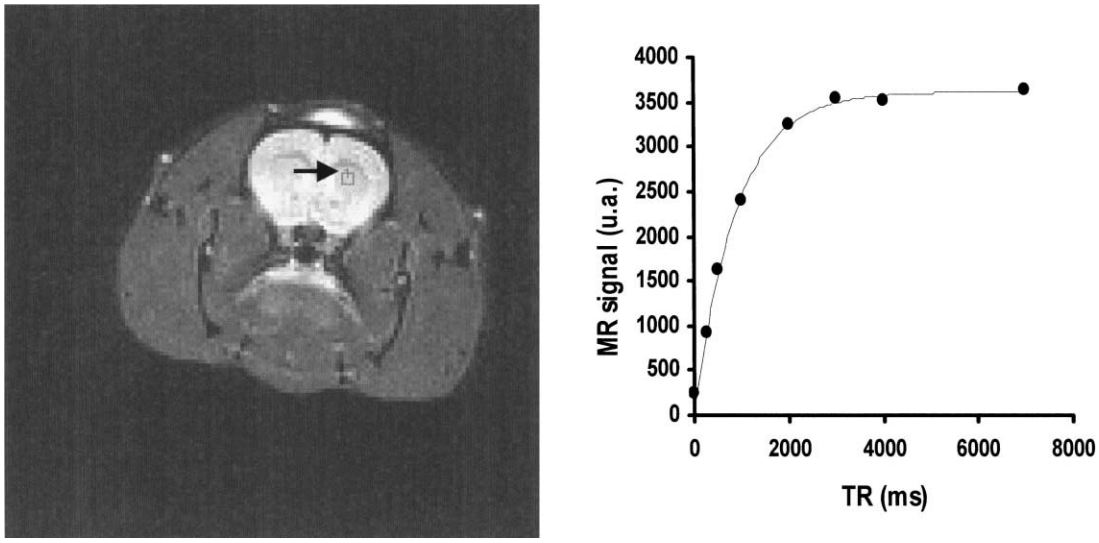

Fig. 1. Determination of the T_1 relaxation time in alive rats. On the left: typical MR image obtained in the rat brain obtained using a fast spin echo (RARE) pulse sequence. A region of interest is indicated by an arrow (here, in the striatum). On the right: fitting of the T_1 corresponding to the region of interest.

surgical blades and well mixed before amounts of 200–300 mg of wet tissue were sampled and weighed into quartz metal free digestion vials; for the striatum the total amount of freshly dissected tissue, i.e. 50–80 mg were weighed. The 0.5 ml of 65% HNO_3 (Merck ultra pure) was added to each digestion vial and the volume completed to 5 ml with ultra pure water. The mixture was mineralized in a microwave digester using the program for fatty materials (sample preparation system, Paar Physica). The resulting clear solutions were adjusted to 10 ml with ultra pure water and analyzed by AAS using a Perkin-Elmer GFAAS, model 5100, equipped with a HGA graphite furnace and a Zeeman-effect background correction system (Mn detection wavelength: 279.5 nm). AAS measurements were performed by comparison with a calibration line of Mn^{2+} standard solutions in diluted HNO_3 (about 0.1 mol/l) ranging from 3 to 9 μg Mn/l. The AAS Mn results of the brain tissues were expressed in μg Mn/g wet weight (w.w.) of tissue.

RESULTS

Metal-Doped Rat Brain Homogenates

The relaxation rates R_1 ($1/T_1$) were plotted as a function of the metal ion (Mn^{2+}, Fe^{3+}, Cu^{2+}) concentration (Fig. 2). As seen in Fig. 2, iron (Fe^{3+}) and copper (Cu^{2+}) had a negligible effect on the relaxation rates of the brain homogenates at the low concentrations tested (at 37°C and 4.7 T). On the contrary, Mn^{2+} dramatically decreased the relaxation times of the brain homogenates and a linear relationship was established between the Mn concentration and the relaxation rates (correlation coefficient $r = 0.98$; $P < 0.01\%$; $n = 14$) (Fig. 2).

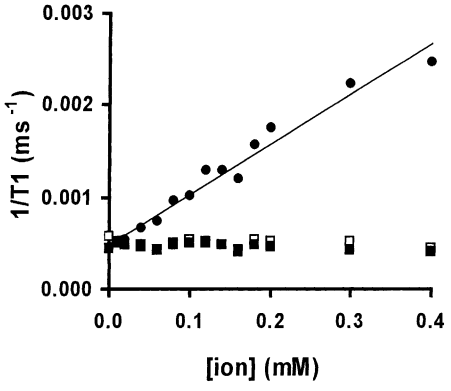

Fig. 2. Influence of increasing amounts of metal ions (●: Mn^{2+}; ■: Cu^{2+}; □: Fe^{3+}) added to rat brain homogenates on the proton relaxation rates ($1/T_1$).

Rat Model for Mn Neurotoxicity

The in vivo results obtained in 29 rats (Fig. 3) demonstrated a strong dependence of the relaxation time T_1 as a function of the Mn concentration determined by AAS. The linear dependence of these two parameters showed for the striatum, the cortex, and the cerebellum correlation coefficients ($r = 0.84$; $P < 0.01\%$; $n = 29$), ($r = 0.77$; $P < 0.01\%$; $n = 29$), and

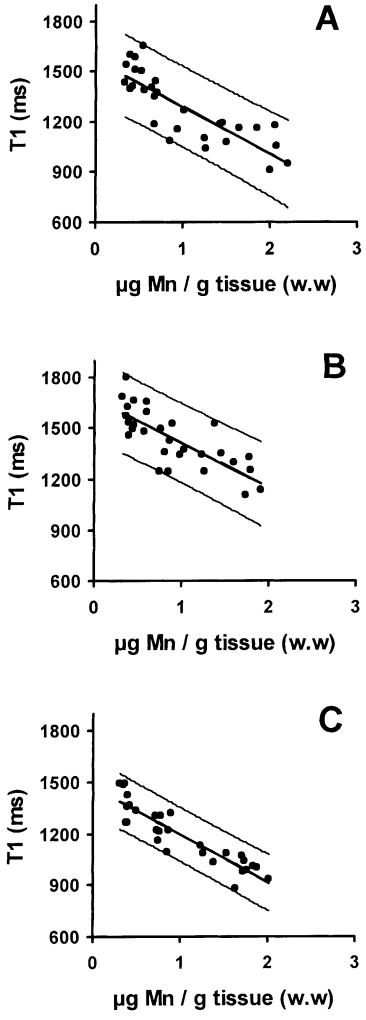

Fig. 3. In vivo results obtained in 29 rats after stereotactical injection with increasing amounts of Mn^{2+} in the ventricles. Proton relaxation times in three brain sites as a function of the tissue Mn concentration determined by AAS. The results indicate a linear dependence between these two parameters: (A) striatum ($r = 0.84$; $P < 0.01\%$; intercept: 1571 ms; slope: −283); (B) cortex ($r = 0.77$; $P < 0.01\%$; intercept: 1675 ms; slope: −262) and (C): cerebellum ($r = 0.92$; $P < 0.01\%$; intercept: 1475 ms; slope: −279). The 95% confidence bands for individual observations are shown.

($r = 0.92$; $P < 0.01\%$; $n = 28$), respectively. In the control rats, the basal concentrations of Mn (mean± S.E.) determined by AAS were 0.436 ± 0.024 μg Mn/g w.w. for the striatum, 0.400 ± 0.015 μg Mn/g w.w. for the cortex, and 0.391 ± 0.051 μg Mn/g w.w. for the cerebellum and were in line with data from the literature (Roels et al., 1997). In our rat model and at 4.7 T, the physiological values of T_1 (control rats) were 1510 ± 89 (mean ± S.D.), 1588 ± 108, and 1380 ± 92 ms for the striatum, the cortex and the cerebellum, respectively.

DISCUSSION

Up to now, there is no non invasive reliable biomarker for the concentration of Mn in the brain after intoxication to this metal. The method described in the present paper provides an appropriate standardization method: local measurement of T_1 provides a quantitative estimation of the concentration of Mn found in different brain regions. This tool will be especially useful for studies on animals in determining non invasively the effect of different routes of administration for the Mn, and in monitoring on the same animals the efficacy of treatments aimed at decreasing the level of the metal in the brain.

It should be a major advance to transpose this quantitative method in patients because, up to now, only subjective MRI scores have been described to assess the degree of Mn intoxication in patients. Before this method will be useful in the clinical situations, there will be a need for further investigations on specific areas including: (1) importance of the magnetic field used (Koenig et al., 1985; Gallez et al., 1996); (2) influence of other metals on the NMR relaxation times.

We would like to emphasize the importance of the magnetic field used for the measurements of NMR relaxation times. Indeed, T_1 depends on the magnetic field and this is especially important for Mn^{2+} as this ion is 'immobilized' by interaction(s) with proteins which leads to a characteristic nuclear magnetic resonance dispersion (NMRD) profile and important variations in the relaxation rates as a function of the magnetic fields used in clinical practice (Koenig et al., 1985; Gallez et al., 1996). Practically, there will be a need for building a standard calibration curve at any magnetic field used.

The specificity of the methodology for Mn intoxication is another important issue. In rat brain homogenates (at 37°C and 4.7 T), Mn^{2+} was identified as the most efficient relaxing ion compared with paramagnetic Cu^{2+} and Fe^{3+} (Fig. 2). This higher relaxivity can be attributed to a high affinity of the Mn ion for proteins with the consequent enhancement in the relaxivity observed at high magnetic field, as it was previously demonstrated using NMRD profiles (Koenig et al., 1985; Gallez et al., 1996). Other factors such as the number of water-binding sites in the metal solvation sphere and the water–metal distance of approach can also have a significant impact on paramagnetic enhancement. The fact that Mn has a greater effect as relaxing ion is essential if we consider future clinical applications of this methodology. It has previously been assumed that the MR signal hyperintensities observed in the corpus striatum of patients were due to the influence of the paramagnetic Mn^{2+} ion. While this assumption is reasonable for workers exposed to Mn dust or for experimental Mn neurotoxicity models in animal, the assumption is more questionable for cirrhotic patients, whose homeostasis of other metal ions (viz. copper and iron) may also be impaired. However, as the MR signal hyperintensity observed in the brain positively correlated with erythrocyte Mn concentration (Malecki et al., 1999), it was reasonable to consider that the MR abnormalities were mainly due to the presence of Mn deposits in the brain. That Mn^{2+} is by far more efficient than Cu^{2+} and Fe^{3+} for decreasing the proton relaxation times (Fig. 2) reinforces the fact that T_1 changes observed in the brain are probably due to the presence of Mn^{2+} ions. In order to definitively demonstrate the specificity of the method for Mn in clinical situations, there will also be a need for comparing the effect of relevant concentrations of different metals in vivo at the magnetic field used in clinic.

CONCLUSION

We have described a method which provides a non invasive and quantitative estimation of Mn ion. This is a unique tool for monitoring the Mn concentration in animal models. We are further investigating the possibility to transpose this methodology in the clinical situations for monitoring the degree of intoxication of Mn-exposed workers.

ACKNOWLEDGEMENTS

This work is supported by the Fonds de la Recherche Scientifique Médicale, FRSM convention 3.4589.99 (National Fund for Scientific Research, Belgium).

REFERENCES

Barbeau A. Manganese and extrapyramidal disorders. NeuroToxicology 1984;5:13–36.

Gallez B, Bacic G, Swartz HM. Evidence for the dissociation of the hepatobiliary MRI contrast agent Mn–DPDP. Magn Reson Med 1996;35:14–9.

Gallez B, Baudelet C, Adline J, Geurts M, Delzenne N. Accumulation of manganese in the brain of mice after intravenous injection of manganese-based contrast agents. Chem Res Toxicol 1997;10:360–3.

Gallez B, Baudelet C, Geurts M. Regional distribution of manganese found in the brain after injection of a single dose of manganese-based contrast agents. Magn Reson Imaging 1998;16:1211–5.

Hauser RA, Zesiewicz TA, Rosemurgy AS, Martinez C, Olanow CW. Manganese intoxication and chronic liver failure. Ann Neurol 1994;36:871–5.

Huang CC, Chu NS, Lu CS, Wang JD, Tsai JL, Tzeng JL, Wolters EC, Calne DB. Chronic manganese intoxication. Arch Neurol 1989;46:1104–6.

Kim SH, Chang KH, Chi JG, Cheong HK, Kim JY, Kim YM, Han MH. Sequential changes of MR signal intensity of the brain after manganese administration in rabbits. Invest Radiol 1999;34:383–93.

Koenig SH, Brown RD, Goldstein EJ, Burnett KR, Wolf GL. Magnetic field dependence of proton relaxation rates in tissues with added Mn^{2+}: rabbit liver and kidney. Magn Reson Med 1985;2:159–69.

Krieger D, Krieger S, Jansen O, Gass P, Theilmann L, Lichtnecker H. Manganese and chronic hepatic encephalopathy. Lancet 1995;346:270–4.

Malecki EA, Devenyi AG, Barron TF, Mosher TJ, Eslinger P, Flaherty-Craig CV, Rossaro L. Iron and manganese homeostasis in chronic liver disease: relationship to pallidal T_1-weighted magnetic resonance signal hyperintensity. NeuroToxicology 1999;20:647–52.

Mergler D. Manganese: the controversial metal. At what levels can deleterious effects occur? Can J Neurol Sci 1996;23:93–4.

Mirowitz SA, Westrich TJ. Basal ganglia signal intensity alterations: reversal after discontinuation of parenteral manganese administration. Radiology 1992;185:535–6.

Nelson K, Golnick J, Korn T, Angle C. Manganese encephalopathy: utility of early magnetic resonance imaging. Br J Ind Med 1993;50:510–3.

Newland MC, Weiss B. Persistent effects of manganese on effortful responding and their relationship to manganese accumulation in the primate globus pallidus. Toxicol Appl Pharmacol 1992;113:87–97.

Newland MC, Ceckler TL, Kordower JH, Weiss B. Visualizing manganese in the primate basal ganglia with magnetic resonance imaging. Exp Neurol 1989;106:251–8.

Pautler RG, Silva AC, Koretsky AP. In vivo neuronal tract tracing using manganese-enhanced magnetic resonance imaging. Magn Reson Med 1998;40:740–8.

Roels HA, Ghyselen P, Buchet JP, Ceulemans E, Lauwerys RR. Assessment of permissible exposure level to manganese in workers exposed to manganese dioxide dust. Br J Ind Med 1992;46:25–34.

Roels H, Meiers G, Delos M, Ortega I, Lauwerys R, Buchet JP, Lison D. Influence of the route of administration and the chemical form ($MnCl_2$, MnO_2) on the absorption and cerebral distribution of manganese in rats. Arch Toxicol 1997;71:223–30.

Roels HA, Ortega Eslava MI, Ceulemans E, Robert A, Lison D. Prospective study on the reversibility of neurobehavioral effects in workers exposed to manganese dioxide. NeuroToxicology 1999;20:255–72.

Shinotoh H, Snow BJ, Hewitt KA, Pate BD, Doudet D, Nugent R, Perl DP, Olanow W, Calne DB. MRI and PET studies of manganese-intoxicated monkeys. Neurology 1995;45:1199–204.

Spahr L, Butterworth R, Fontaine S, Bui L, Thierren G, Milette P, Lebrun L. Increased blood manganese in cirrhotic patients: relationship to pallidal magnetic resonance signal hyperintensity and neurological symptoms. Hepatology 1996;24:1116–20.